Autonomous Surface Vehicle Swarms with Bifurcation-driven Multi-behavioral Dynamics

Kleio Baxevani, Chanaka Thushitha Bandara, Herbert G. Tanner

***Abstract*— This paper outlines an approach to coordinating collections of autonomous marine surface vehicles and enable them to exhibit different group behaviors in a way that does not necessitate analysis using switched or hybrid system formulations. Instead, the group behaviors are generated using reference vector fields which are created through a single underlying dynamical system that undergoes bifurcations. The benefits of such an approach can be both theoretical and practical: on one hand the formulation obviates the need for a combinatorial or switched system theoretical analysis in order to reliably predict and guarantee overall system properties, and on the other it is applicable to multi-robot systems that lack the capability for direct robot-to-robot sensing or communication. The ability of such a formulation to generate two key group behaviors, namely, a cyclic pursuit and a convergence to target, is validated both numerically as well as experimentally using a small fleet of Jaiabot micro-AUVs.**

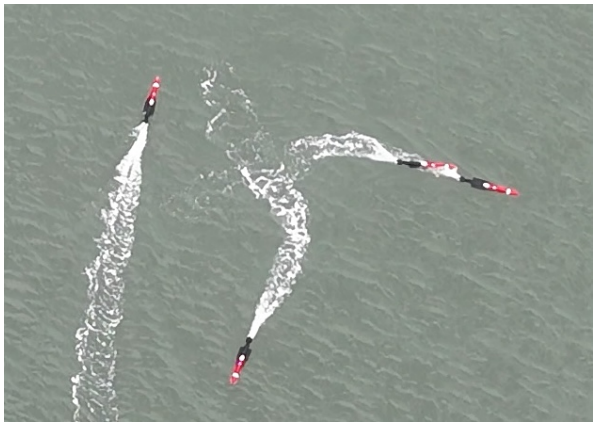

Fig. 1: A small fleet of four Jaiabots as they reconfigure themselves to achieve a group control objective.

I. INTRODUCTION

Environmental monitoring and in-situ measurement in marine environments, in particular, is becoming increasingly crucial due to the growing impacts of climate change on ocean ecosystems, such as rising in sea levels, marine life, and water quality. Accurate and timely monitoring is essential for understanding these changes, guiding conservation efforts, and developing strategies to mitigate environmental impacts [1], [2]. Traditional observation methods, which primarily rely on in-situ measurements from stationary platforms, are constrained by high costs and limited spatial coverage. Suck tasks can be mentally exhausting and error-prone for humans, leading to decreased productivity and increased fatigue due to their repetitive nature. This can be resolved by automating these dull tasks and using *one or multiple autonomous marine vehicles* to perform repetitive, monotonous work with precision and consistency.

The prospect of autonomously deploying *swarms* of marine vehicles is appealing from the perspective of scaling up and accelerating observation, monitoring, and mapping missions. By now there is a wealth of biologically-inspired algorithms for robot flocking and swarming, which will not be attempted to be reviewed and referenced in this short paper. The beauty of the nearest-neighbor interaction paradigm on which this body of literature is based is its simplicity and scalability. Multi-agent systems that converge to a moving geometric formation around a target have predominantly relied on local interactions [3], [4] while often utilizing strategies that enforce constant inter-agent bearing [5], [6]. Extensions of these methods include using a fixed beacon as a reference point [7] to regulate the position of the circumcenter and the radius of the circular orbit. Elements of bifurcation theory have also been utilized to form such patterns [8], [9]; the challenge, however, lies in its implicit assumption that the robot swarm members can either communicate with or sense the motion of each other.

None of these two potential assumptions is (currently) valid for the commercially available Jaiabot micro-autonomous underwater vehicle (AUV) platform featured in Fig. 1. This is not a singularity; in fact there are other instances of robot collectives, at many different scales, which lack the capacity for these two type of functions [10], [11]. For robot system collectives that are subject to these type of resource constraints, a scalable multi-robot coordination solution can be offered in the form of *reference vector fields*, which serve as a feedback-based mechanism to suggest to all robots a desired direction of motion based on each individual robot's location. Technologies capable of generating such artificial (or natural) vector fields that can steer a collection of robots have been reported in the literature [12]–[14]. Considering the no inter-agent communication, this Eulerian approach akin to [15] acts as a universal feedback law broadcast by a central supervisor that can more easily be tackled with existing design and analysis tools (e.g. [16]), and with a significant benefit of resilience and robustness. One limitation, however, is that a vector field of this nature will typically capture a *single* collective behavior, and if the swarm needs to switch to a different behavior then a different vector field needs to be activated.

Baxevani is with the Department of Aerospace Engineering at the University of Maryland. Bandara, and Tanner are with the Center for Autonomous and Robotic Systems (CARS) at the University of Delaware; Email: kleio@umd.edu, {chanaka, btanner}@udel.edu.

This work was supported by USGS via award #G23AC00149-00 and NOAA's Project ABLE via award #NA22OAR4690620-T1-01

This is always possible in the theoretical context of switched or hybrid systems [17]–[19]. Yet, establishing fundamental properties such as existence and uniqueness of solutions, robustness, stability, and continuity with respect to initial conditions and parameters is considerably more complex in a hybrid system compared to a continuous dynamical system [20] and that complexity increases with the dimensionality of the multi-agent system.

An alternative route is bifurcation-based vector fields [21], [22]. These approaches realize the potential of tunable navigational dynamics to steer a collective of agents while switching their dynamical behavior using certain types of bifurcations such as Hopf bifurcation. However, testing and validation of these approaches have been so far done in simulation or controlled lab environments, and thus, there is no evidence of the efficacy of such methods in *field conditions.*

In an attempt to narrow this gap, this work explores the application of bifurcation theory to develop multi-behavioral autonomous surface vehicles (ASVs). We propose a framework that leverages the theoretical insights of bifurcation theory to enhance the coordination and collective behavior of ASVs without necessitating direct communication between agents. Such a framework can enable two types of behaviors without modifying the underlying system dynamics: a repetitive task or limit cycle behavior and a convergence-to-point behavior. Limit cycle behaviors are useful in patrolling or coverage missions, whereas point convergence is useful for rallying the vehicles, e.g., for recovery. There are various types of autonomous marine vehicles well-suited for such applications, each equipped with different payloads and sensors [23]–[26], however, there is still room for improvement in multi-robot coordination and control in marine environments.

The rest of the paper is organized as follows. Initially, a brief overview of the system architecture is provided in Section II followed by Section III, which introduces the mathematical description of the vehicle kinematics along with the main technical results of the paper. In Section IV, the performance of the proposed method is evaluated numerically and through simulations, and after laying out the hardware and software tools employed for this integration, the section closes with the preliminary field testing results. Finally, Section V provides a brief summary of the paper and emphasizes the potential impact of the proposed approach on the marine robotics industry.

II. Overview of the System

The proposed framework was tested in the real world using the *Jaiabot*, a micro ASV specifically designed for environmental monitoring (see Fig. 2) [27], [28]. The Jaiabot, approximately one meter long and weighing 3 kg, features a torpedo-like design and is capable of reaching speeds up to 5 m/s with a range of 11 km. In addition to its primary role as an ASV, the Jaiabot can perform vertical dives, is propelled by a single propeller, and is steered using a rudder. Equipped with sensors for measuring salinity, temperature, and depth, and rated for operations at depths of up to 30 m, the Jaiabot represents a versatile tool for environmental monitoring. The platform can be controlled manually or autonomously using the Jaia Command and Control graphical user interface (GUI), however, the system currently lacks inter-agent communication capabilities, highlighting the need for further advancements in swarm coordination methodologies.

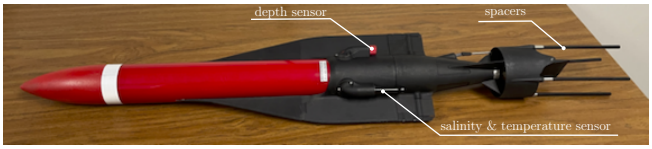

Fig. 2: The Jaiabot micro ASV, by Jaia Robotics can serve as an autonomous platform for environmental monitoring.

An overview of the system is illustrated in Fig. 3. The colored-coded boxes indicate different subsystems of the system architecture, and the arrows show the information flow between them. The onboard processes and hardware are within the orange block, while the nodes inside the green block indicate the processes that occur on the central coordinating computer on shore. The communication between the onboard and on-shore parts of the system is established using a radio antenna with a range of up to 11km in direct view.

The GPS sensor of the system is located on the nose of the vehicle and provides a geolocation position while transiting on the surface that is shared through radio to the GUI and the on-shore computer. Based on the desired task/behavior selected, the path planner module will compute the desired artificial vector field, and given the position information of the vehicle, it will return the desired forward speed and heading to the low-level controller. Finally, the low-level control will translate the speed and heading into the desired RPMs for the thruster and the desired direction for the rudder.

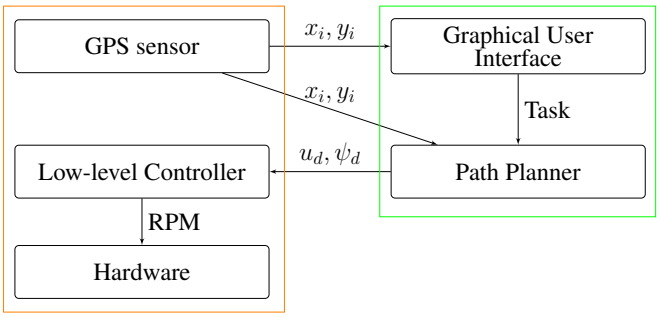

Fig. 3: Block diagram of the system architecture. *In Orange*: The onboard elements of the system which provide the location of the vehicle and translate the desired state of the vehicle into hardware commands. *In Green*: The GUI runs on a ground station desktop on-shore and runs the path planning design for the vehicles.

III. Multi-behavioral Dynamics

A. Vehicle Kinematics

In this work, we consider an ASV with kinematics in three degrees of freedoms (DOFs), surge, sway, and yaw. The generalized positions and velocities can, then, be defined as $\boldsymbol{\eta} = [x,y,\psi]^\intercal$ and $\boldsymbol{\nu} = [u,v,r]^\intercal$, respectively. Thus, the

matrix-vector representation of the craft's kinematics [29] can take the form

$$\dot{\boldsymbol{\eta}} = \underbrace{\begin{bmatrix} \cos\psi & -\sin\psi & 0 \\ \sin\psi & \cos\psi & 0 \\ 0 & 0 & 1 \end{bmatrix}}_{\boldsymbol{R}(\psi)(\psi)} \boldsymbol{\nu} \ . \tag{1}$$

The objective of this paper is to design a feedback law that can alter the system's resulting behavior without changing the underlying dynamics but simply changing the value of a scalar parameter.

B. General Formulation

Let $w = (x, y) \in \mathcal{D} \subseteq \mathbb{R}^2$, and consider *planar vector fields* $F_i(w) : \mathcal{D} \to T\mathcal{D}$, for $i \in I \subset \mathbb{N}$, and $T\mathcal{D}$ represent the tangent bundle of the manifold $\mathcal{D}$. Each vector field has an *associated (Lyapunov) function* $f_i : \mathcal{D} \to \mathbb{R}$ for which it is known that $\dot{f}_i = \nabla^\intercal f_i \, F_i \leq 0$. (Equality on the right holds at the equilibria of F_i.)

Let m_1 and m_2 be scalar variables in $[0, 1]$ representing the degree to which the dynamical behavior captured by F_i manifests itself in the system. These two variables define the *motivation state* of the system; they can have dynamics of their own and thus evolve over time.

The scalar variables v_i, referred to as *values*, encode the importance of each dynamical behavior F_i. The value of a component vector field F_i increases as the urgency of the task/behavior encoded in F_i increases. As with the motivation state, the value state has its own dynamics that will be introduced shortly.

Based on F_i and m_i, the *navigation dynamics* is defined as a dynamical system formed by the convex combination of F_i, using the motivation state variables m_i as weights:

$$\dot{w} = m_1(t) \cdot F_1(w) + m_2(t) \cdot F_2(w) \ . \tag{2}$$

The *value dynamics* is defined as

$$\dot{v}_i = \tfrac{1}{\lambda_i}(f_i - v_i) \ , \tag{3}$$

where λ_i is a scale parameter. Define now the *undecided motivation state* $m_U \triangleq 1 - \sum_i m_i$, and let $\sigma \in \mathbb{R}_+$ be the *bifurcation parameter*, and v_i^* is a positive real gain. Then the *motivation dynamics* of the system inspired by the decision-making behavior in honeybee swarms ([30]) is defined as

$$\dot{m}_i = v_i^* v_i m_U - m_i\big[\tfrac{1}{v_i^* v_i} - v_i^* v_i m_U + \sigma(1 - m_i - m_U)\big] \ . \tag{4}$$

With this dynamical system setup in place, define the set of *mean-difference* coordinates

$$\bar{F} = \tfrac{F_1(w)+F_2(w)}{2} \qquad \Delta F = F_1(w) - F_2(w) \tag{5a}$$
$$\bar{f} = \tfrac{f_1(w)+f_2(w)}{2} \qquad \Delta f = f_1(w) - f_2(w) \tag{5b}$$
$$\bar{m} = \tfrac{m_1(t)+m_2(t)}{2} \qquad \Delta m = m_1(t) - m_2(t) \tag{5c}$$
$$\bar{v} = \tfrac{v_1(t)+v_2(t)}{2} \qquad \Delta v = v_1(t) - v_2(t) \ , \tag{5d}$$

which can be combined into a stack vector

$$q = (x, y, \bar{m}, \Delta m, \bar{v}, \Delta v)^\intercal \ . \tag{6}$$

C. Particular Instantiation

Now assume, for clarity of presentation, that we have just two planar vector fields of the form:

$$\dot{x} = r(y - y_{ci}) - (x - x_{ci})\big[(x - x_{ci})^2 + (y - y_{ci})^2 - r^2\big]$$
$$\dot{y} = -r(x - x_{ci}) - (y - y_{ci})\big[(x - x_{ci})^2 + (y - y_{ci})^2 - r^2\big]$$

which each produces a circular attractive limit cycle centered at (x_{ci}, y_{ci}) and with radius $r > 0$.

Without loss of generality, we can simplify the analysis assuming: $(x_{c_1}, y_{c_1}) = (0, 0)$, $y_{c_2} = 0$, and $x_{c_2} \triangleq x_{\text{dis}} > 0$, which reduces the expressions of the vector fields to the form:

$$F_1 : \begin{cases} \dot{x} = ry - x(x^2 + y^2 - r^2) \\ \dot{y} = -rx - y(x^2 + y^2 - r^2) \end{cases} \tag{7a}$$

$$F_2 : \begin{cases} \dot{x} = ry - (x - x_{\text{dis}})[(x - x_{\text{dis}})^2 + y^2 - r^2] \\ \dot{y} = -r(x - x_{\text{dis}}) - y[(x - x_{\text{dis}})^2 + y^2 - r^2] \end{cases} , \tag{7b}$$

from which we can define *associated Lyapunov functions* $f_i(x, y)$ as follows:

$$f_1(x, y) = \tfrac{1}{4}(x^2 + y^2 - r^2)^4 \tag{8a}$$
$$f_2(x, y) = \tfrac{1}{4}\big[(x - x_{\text{dis}})^2 + y^2 - r^2\big]^4 \ . \tag{8b}$$

The dynamics of the mean-difference coordinates induced by (2)–(4) after substituting (7) and (8) can be expressed as—with a slight abuse of notation where we use $(\dot{x}, \dot{y})$ to express the components of the blended vector field $\dot{w}$ in (2):

$$\begin{aligned} \dot{w}_1 \equiv \dot{x} = \Delta m \, x_{\text{dis}}(0.5r^2 - 1.5x^2 + 1.5x_{\text{dis}}x - 0.5y^2 \\ - 0.5x_{\text{dis}}^2) + \bar{m}(r^2(2x - x_{\text{dis}}) + 2ry - 2x^3 \\ + 3x^2 x_{\text{dis}} - 2xy^2 - 3x_{\text{dis}}^2 x + y^2 x_{\text{dis}} + x_{\text{dis}}^3) \end{aligned} \tag{9a}$$

$$\begin{aligned} \dot{w}_2 \equiv \dot{y} = \ \Delta m \, x_{\text{dis}}(-0.5r - xy + 0.5yx_{\text{dis}}) + \bar{m}(2r^2 y \\ - 2rx + rx_{\text{dis}} - 2x^2 y + 2xyx_{\text{dis}} - 2y^3 - yx_{\text{dis}}^2) \end{aligned} \tag{9b}$$

$$\begin{aligned} \dot{\bar{m}} = \ 0.25\sigma(\Delta m^2 - 4\bar{m}^2) + \tfrac{0.25\Delta m \Delta v(1-2\bar{m})}{\epsilon_m} \\ - \tfrac{0.5\epsilon_m(\Delta m + 2\bar{m})}{2\bar{v} + \Delta v} + \tfrac{0.5\epsilon_m(\Delta m - 2\bar{m})}{2\bar{v} - \Delta v} + \tfrac{\bar{v}(1-2\bar{m})(\bar{m}+1)}{\epsilon_m} \end{aligned} \tag{9c}$$

$$\begin{aligned} \tfrac{\mathrm{d}\Delta m}{\mathrm{d}t} = -\tfrac{\epsilon_m(\Delta m + 2\bar{m})}{2\bar{v} + \Delta v} - \tfrac{\epsilon_m(\Delta m - 2\bar{m})}{2\bar{v} - \Delta v} \\ - \tfrac{\bar{v}\Delta m(2\bar{m}-1)}{\epsilon_m} - \tfrac{\Delta v(2\bar{m}^2 + \bar{m} - 1)}{\epsilon_m} \end{aligned} \tag{9d}$$

$$\dot{\bar{v}} = \tfrac{1}{\epsilon_v}(\bar{f} - \bar{v}) \tag{9e}$$

$$\frac{\mathrm{d}\Delta v}{\mathrm{d}t} = \tfrac{1}{\epsilon_v}(\Delta f - \Delta v) \ , \tag{9f}$$

setting $v_1^* = v_2^* = v^*, \lambda_1 = \lambda_2 = \lambda$. The navigation dynamics after solving this system [21] are

$$\dot{w}_1 = w_3 x_{\text{dis}}\big(\tfrac{1}{2}r^2 - \tfrac{3}{2}w_1^2 + \tfrac{3}{2}w_1 x_{\text{dis}} - \tfrac{1}{2}w_2^2 - \tfrac{1}{2}x_{\text{dis}}^2\big) + \tfrac{1}{2}\big[r^2(2w_1 - x_{\text{dis}}) + 2rw_2 - 2w_1^3 + 3w_1^2 x_{\text{dis}} - 2w_1 w_2^2 - 3w_1 x_{\text{dis}}^2 + w_2^2 w_1 + x_{\text{dis}}^3\big] \quad (10a)$$

$$\dot{w}_2 = -w_3 x_{\text{dis}}\big(\tfrac{1}{2}r + w_1 w_2 - \tfrac{1}{2}w_2 x_{\text{dis}}\big) + \tfrac{1}{2}\big(2r^2 w_2 - 2rw_1 + rx_{\text{dis}} - 2w_1^2\tilde{w}_2 + 2w_1 w_2 x_{\text{dis}} - 2w_2^3 - w_2 x_{\text{dis}}^2\big) \quad (10b)$$

$$\dot{w}_3 = -\bar{f} w_3 \tfrac{\sigma(w_3^2-1)}{w_3\Delta f + 3\bar{f}} - \tfrac{3}{4}\Delta f \tfrac{\sigma(w_3^2-1)}{w_3\Delta f + 3\bar{f}} \ , \quad (10c)$$

where the pair (w_1, w_2) corresponds to the (x, y) dynamics.

D. Vector Field Transformation

In order to transfer this mathematical analysis into the real world, some adjustments were necessary. More specifically, we performed a scale transformation and a translation to the mathematically resulting trajectories based on the point of interest (deadlock), the area we would like to patrol, and the turning radius of the robotic platform. Our final system evolves around the deadlock, which can be moved to the origin without loss of generality and then, transformed the coordinates of the trajectory from Cartesian (x, y) to polar coordinates (ρ, θ).

$$\begin{cases} x' = x - x_d \\ y' = y - y_d \end{cases} \xrightarrow[\text{coordinates}]{\text{Polar}} \begin{cases} \rho = \sqrt{x'^2 + y'^2} \\ \theta = \tan^{-1}\frac{y'}{x'} \end{cases} \quad (11a)$$

$$\xrightarrow[\text{by term } \tau]{\text{Scaling}} \begin{cases} \rho' = \tau\rho \\ \theta' = \theta \end{cases} \quad (11b)$$

$$\xrightarrow[\text{coordinates}]{\text{Cartesian}} \begin{cases} x'' = \tau x' \\ y'' = \tau y' \end{cases} . \quad (11c)$$

IV. Validation

The performance validation below considers combining two vector fields admitting circular limit cycles and parameterized with $x_{\text{dis}} = 2.5$ and $r = 1.4$. Then, there should be a deadlock located at $\tilde{w}_d = (1.25, 0)^\intercal$; after substituting $(x_{\text{dis}}, r) = (2.5, 1.4)$, in the analytical form for σ, the critical bifurcation parameter is found to be $\sigma_c = 0.0434$ [21].

A. Numerical Validation

Before translating the resulting dynamics into the corresponding software for the robotic platforms, we verified them via numerical simulations shown in Fig. 4 and Fig. 5. In this numerical example, we identify the point of interest as $(2, 1)$ and the area of interest as spanning the range $x \in [-3, 7]$ and $y \in [-9, 11]$. This requirement implies that our deadlock should be translated to $(2, 1)$ and scale up the resulting limit cycle around it in the defined range by a scaling parameter $\tau = 50$ while maintaining the behavioral characteristics of the system. By setting the bifurcation parameter above the critical value (Fig. 4), the system will evolve in a periodic orbit around the desired point of interest $(2, 1)$ and within the desired area shown with dashed lines. On the other end, when we set the bifurcation parameter below the critical value then the system will converge to the point of interest and settle there for the remaining evolution time (Fig. 5).

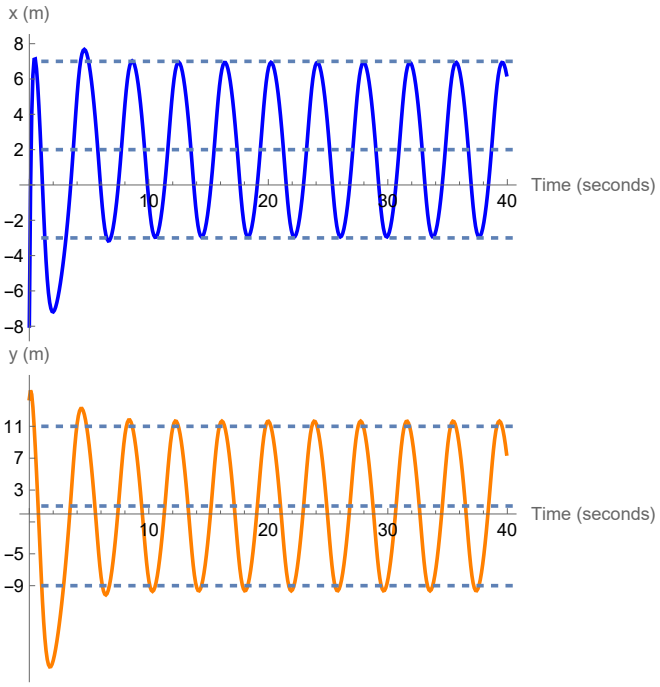

Fig. 4: Numerical time evolution of the x and y dynamics when the bifurcation parameter is set above the critical value $\sigma = 0.1 > \sigma_{cr}$.

B. Simulation

To transfer the mathematical analysis into the ASV kinematics, we use the Jaia Command and Control Interface developed by Jaia Robotics (Fig. 6). That is the GUI used for the simulation analysis and the field testing. In this example, we include four jaiabots in the simulation environment operating in the University of Delaware Marine Operation facilities in Lewes, DE. The square area in Fig. 6 indicates the operationally safe area of interest the agents need to patrol. First, the agents are instructed to patrol the area by setting the bifurcation value above the critical value $(\sigma = 0.1 > \sigma_{cr})$ for 300 seconds. The geolocation of each agent is provided by the GPS antenna at the front part of the platform and translated into the system coordinates, with the origin of that system being the location of the central coordinator on shore (HUB). To demonstrate the different behaviors in an easily comparable way and without loss of generality, we plot the trajectories around the origin instead.

Similar to the numerical validation, we present how the trajectories of the four agents evolve over time with different values of the bifurcation parameter. To cover the desired area, we set the scaling parameter $\tau = 20$. In Fig. 7, we set the bifurcation parameter above the critical value $(\sigma = 0.1)$, and the four agents perform a limit cycle with the x evolving between $[-5, 5]$ and y evolving between $[-7, 7]$. Then, the bifurcation parameter is set below the critical value $(\sigma = 0.01)$, and the four agents converge to a tighter circle where the x evolves between $[-4, 4]$ and y evolves between $[-3, 3]$ as shown in Fig. 8. Note that an attractive deadlock is a focus,

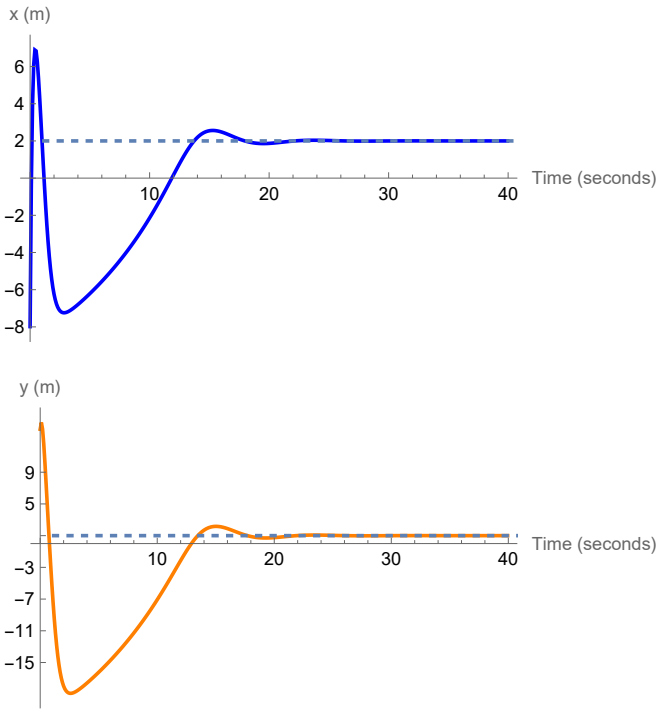

Fig. 5: Numerical time evolution of the x and y dynamics when the bifurcation parameter is set below the critical value $\sigma = 0.01 < \sigma_{cr}$.

which means that the vector field flow lines that converge to it will spiral in. However, the Jaiabot being steered via a thruster and a rudder, has a minimum turning radius. For that reason, as it follows this vector field, it will end up circling around the deadlock. The radius of this circle is noticeably smaller than that of the limit cycle, thus distinguishing the two collective behaviors.

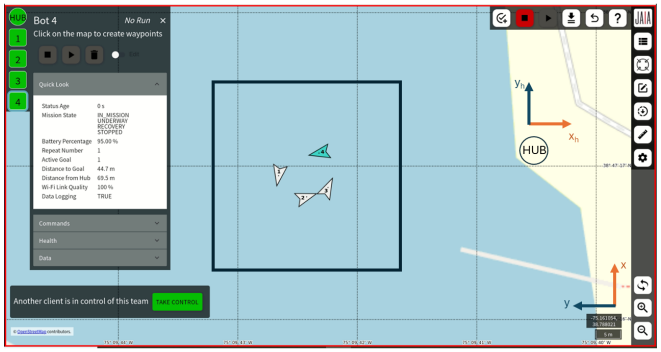

Fig. 6: Screenshot of Jaia Robotics graphical user interface simulating the Marine Operation boat basin of University of Delaware in Lewes, DE, USA. The square area represents the area of interest where the four robots patrol.

C. Field Testing

The preliminary field testing was conducted at the University of Delaware Marine Operations' boat basin in Lewes, DE, using four Jaiabot micro-ASVs. The scenario tested was the same as the simulation scenario. The safe area of interest for the platforms to cover was a square area of 400 m^2. For

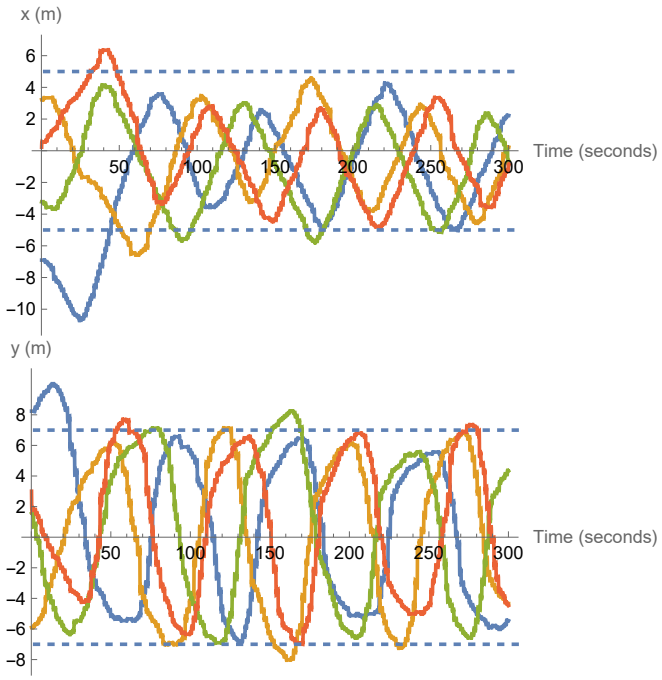

Fig. 7: Evolution of the simulated x and y trajectories of four agents when the bifurcation parameter is above the critical value $\sigma = 0.15 > \sigma_{cr}$.

that reason, the scaling parameter for the field testing was set at $\tau = 50$.

After placing the four Jaiabot ASVs in the water, we directed them to follow a periodic orbit (limit cycle) and patrol the boundary of the area for 300 seconds via setting the bifurcation parameter above the critical value (Fig. 9). After they complete their first task, the bifurcation parameter was set below the critical value which instructed the group to perform a convergent task around a point of interest (convergence to a point) for another 300 seconds (Fig. 10). As in the simulation example, the trajectories have been translated around the origin to make the comparison between the two tasks more apparent.

The recorded trajectories are admittedly noisy; this is due not only to the lag of communication between the central computer and the platforms but primarily so because of the measurement error of the GPS sensor. Nevertheless, the periodicity of the steady-state behaviors is visible. Similar to the simulation results, the difference between the two behaviors is highlighted by noticing the difference in the radius of the trajectories. In the case of the patrolling task, the x and y trajectories approximately span between $[-15, 15]$, while in the second case, they span between $[-6, 6]$, with the latter being due to turning radius constraint of the vehicles as explained above. Through these results, we can verify the applicability of bifurcation based multi-behavioral dynamics in a non-sterile field environment.

V. Conclusion

This work demonstrates the feasibility of the development and deployment of an alternative multi-behavioral path planning design. This approach utilizes elements from bifurcation

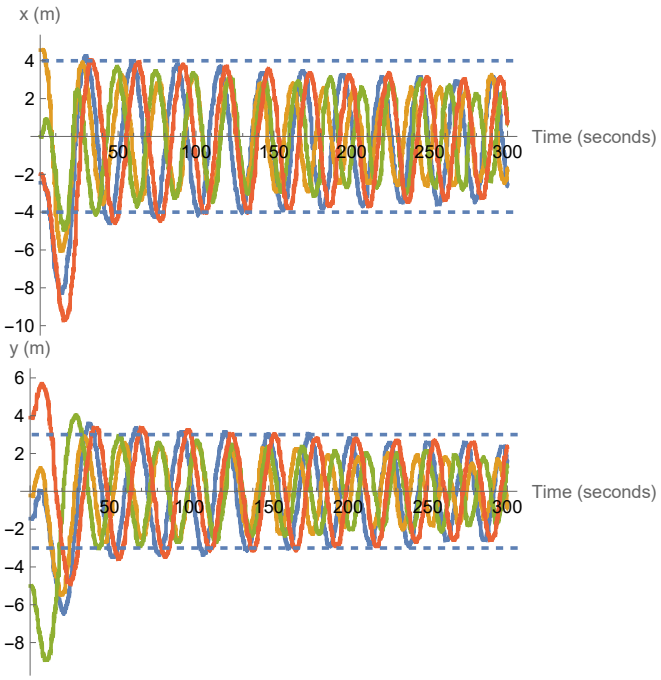

Fig. 8: Evolution of the simulated x and y trajectories of four agents when the bifurcation parameter is set below the critical value $\sigma = 0.01 < \sigma_{cr}$.

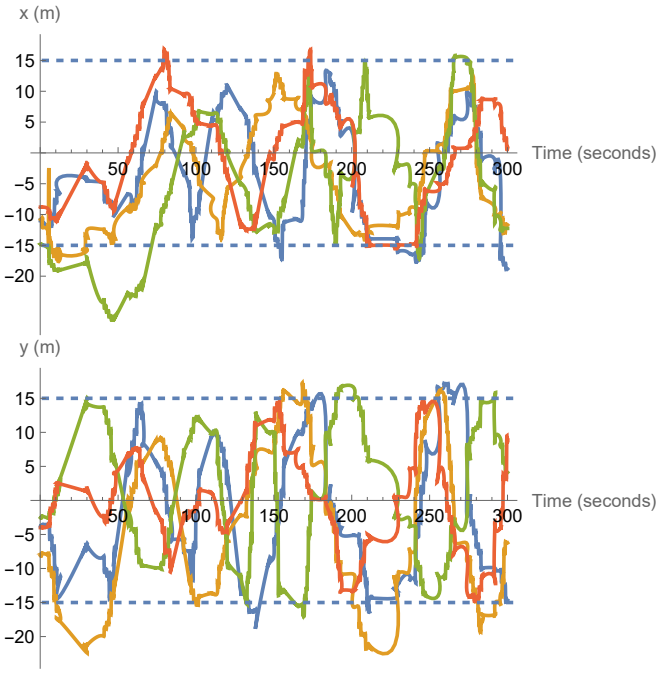

Fig. 9: Evolution of the x and y trajectories of the four Jaiabots performing a limit cycle during the field implementation with bifurcation parameter set above the critical value $\sigma = 0.1 > \sigma_{cr}$.

theory and can provide different artificial vector fields that can steer a collective of ASVs to different behaviors. The underlying dynamics of the system remain throughout and the different behaviors are the result of the shift of the bifurcation parameter to values above and below the critical threshold. Numerical and simulation testing confirmed the performance of the system, while preliminary field testing

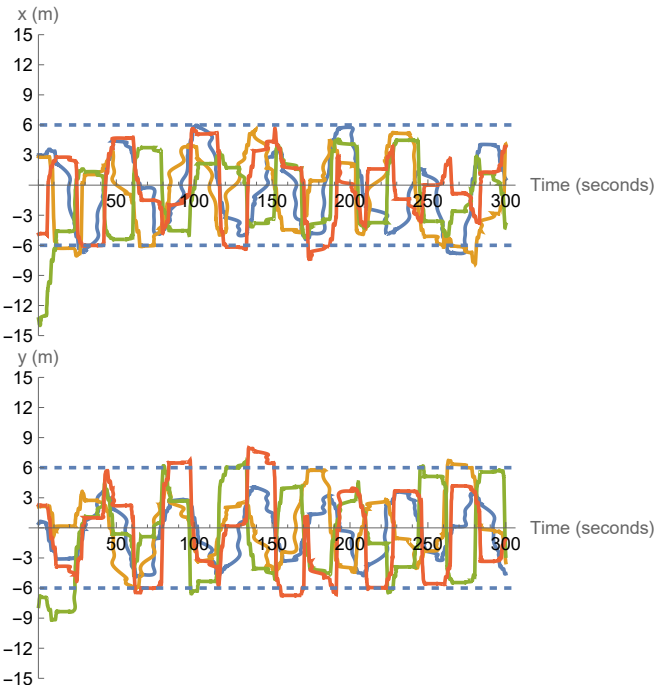

Fig. 10: Evolution of the x and y trajectories of the four Jaiabots converging to their deadlock point during the field implementation with bifurcation parameter set below the critical value $\sigma = 0.01 < \sigma_{cr}$.

was conducted to showcase the different behaviors.

The applicability of this approach is now expanded. After identifying the location of the bifurcation deadlock in the physical world and the size of the safe area for the robots to operate, we provide a method to adjust the resulting system that can exhibit different behaviors around the point of interest while covering the safe area. This new direction expands the capabilities of multi-behavioral multi-agent systems with no inter-agent communications and paves the way for a variety of applications. The proposed results can be applied to any group of homogeneous or heterogeneous platforms that should perform any repetitive behavior, such as sampling and patrolling, or any location-convergent tasks, such as inspecting a point of interest or gathering for recovery.

Acknowledgements

We would like to thank Joshua Mickles, Matthew Ferro, and Michael Rock from Jaia Robotics for assisting us with the hardware, Dr. Arthur Trembanis for giving us access to his lab facilities in Lewes, DE, and Cpt Micheal Birns and his dive team for recovering robots which lost their GPS signal and went out of bounds.

References

[1] Z. Liu, Y. Zhang, X. Yu, and C. Yuan, "Unmanned surface vehicles: An overview of developments and challenges," *Annual Reviews in Control*, vol. 41, pp. 71–93, 2016.

[2] E. Zereik, M. Bibuli, N. Mišković, P. Ridao, and A. Pascoal, "Challenges and future trends in marine robotics," *Annual Reviews in Control*, vol. 46, pp. 350–368, 2018.

[3] L. A. Valbuena Reyes and H. G. Tanner, "Flocking, formation control, and path following for a group of mobile robots," *IEEE Transactions on Control Systems Technology*, vol. 23, no. 4, pp. 1268–1282, 2015.

[4] I. Yadav and H. G. Tanner, "Mobile radiation source interception by aerial robot swarms," in *Proceedings of the 2nd IEEE International Symposium on Multi-Robot and Multi-Agent Systems*, pp. 63–69, 2019.

[5] J. A. Marshall, M. E. Broucke, and B. A. Francis, "Formations of vehicles in cyclic pursuit," *IEEE Transactions on Automatic Control*, vol. 49, no. 11, pp. 1963–1974, 2004.

[6] U. Halder, B. Schlotfeldt, and P. Krishnaprasad, "Steering for beacon pursuit under limited sensing," in *Proceedings of the IEEE 55th Conference on Decision and Control*, pp. 3848–3855, 2016.

[7] K. S. Galloway and B. Dey, "Station keeping through beacon-referenced cyclic pursuit," in *Proceedings of the American Control Conference (ACC)*, pp. 4765–4770, IEEE, 2015.

[8] V. Edwards, P. deZonia, M. A. Hsieh, J. Hindes, I. Triandaf, and I. B. Schwartz, "Delay induced swarm pattern bifurcations in mixed reality experiments," *Chaos: An Interdisciplinary Journal of Nonlinear Science*, vol. 30, no. 7, p. 073126, 2020.

[9] I. B. Schwartz, V. Edwards, S. Kamimoto, K. Kasraie, M. Ani Hsieh, I. Triandaf, and J. Hindes, "Torus bifurcations of large-scale swarms having range dependent communication delay," *Chaos: An Interdisciplinary Journal of Nonlinear Science*, vol. 30, no. 5, p. 051106, 2020.

[10] G. Kouvoutsakis, K. Baxevani, J. Orozco, H. G. Tanner, P. Artemiadis, J. C. Galloway, G. Huang, , and E. Kokkoni, "A pediatric motor training environment based on human-swarm interaction," in *Proceedings of the IEEE International Conference on Development and Learning*, pp. 1–6, 2024.

[11] I. Faros and H. G. Tanner, "An equilibrium analysis of magnetic quadrupole force field with applications to microrobotic swarm coordination," in *Proceedings of the IEEE International Conference on Robotics and Automation*, 2025. (submitted).

[12] H. G. Tanner and A. Boddu, "Multiagent navigation functions revisited," *IEEE Transactions on Robotics*, vol. 28, no. 6, pp. 1346–1359, 2012.

[13] R. Hegde and D. Panagou, "Multi-agent motion planning and coordination in polygonal environments using vector fields and model predictive control," in *2016 European Control Conference (ECC)*, pp. 1856–1861, IEEE, 2016.

[14] H. H. Triharminto, O. Wahyunggoro, T. B. Adji, and A. I. Cahyadi, "An integrated artificial potential field path planning with kinematic control for nonholonomic mobile robot," *International Journal on Advanced Science, Engineering and Information Technology*, vol. 6, no. 4, pp. 410–418, 2016.

[15] P. Kingston and M. Egerstedt, "Index-free multi-agent systems: An eulerian approach," *IFAC Proceedings Volumes*, vol. 43, no. 19, pp. 215–220, 2010.

[16] D. Panagou, H. G. Tanner, and K. J. Kyriakopoulos, "Control of nonholonomic systems using reference vector fields," in *2011 50th IEEE Conference on Decision and Control and European Control Conference*, pp. 2831–2836, IEEE, 2011.

[17] J. Lygeros, K. Johansson, S. Simić, and S. Sastry, "Dynamical properties of hybrid automata," *IEEE Transactions on Automatic Control*, vol. 48, no. 1, pp. 2–17, 2003.

[18] A. J. Van der Schaft and H. Schumacher, *An Introduction to Hybrid Dynamical Systems*. Springer, 2000.

[19] D. Liberzon, *Switching in Systems and Control*. Birkhauser, 2003.

[20] R. Goebel, R. G. Sanfelice, and A. R. Teel, *Hybrid Dynamical Systems*. Princeton University Press, 2012.

[21] K. Baxevani and H. G. Tanner, "Multi-modal swarm coordination via hopf bifurcations," *Journal of Intelligent Robotic Systems*, vol. 109, 2023.

[22] P.-B. Reverdy and D. E. Koditschek, "A dynamical system for prioritizing and coordinating motivations," *SIAM Journal on Applied Dynamical Systems*, vol. 17, no. 2, pp. 1683–1715, 2018.

[23] K. Baxevani, G. E. Otto, A. C. Trembanis, and H. G. Tanner, "Optimal asv path-following for improved marine survey data quality," in *Proceedings of MTS/IEEE OCEANS*, pp. 1–7, 2023.

[24] J. Moulton, N. Karapetyan, S. Bukhsbaum, C. McKinney, S. Malebary, G. Sophocleous, A. Q. Li, and I. Rekleitis, "An autonomous surface vehicle for long term operations," in *Proceedings of MTS/IEEE OCEANS*, pp. 1–10, 2018.

[25] B. Joshi, C. Bandara, I. Poulakakis, H. G. Tanner, and I. Rekleitis, "Hybrid visual inertial odometry for robust underwater estimation," in *Proceedings of the MTS/IEEE OCEANS*, pp. 1–7, 2023.

[26] S. Yuan, Y. Li, F. Bao, H. Xu, Y. Yang, Q. Yan, S. Zhong, H. Yin, J. Xu, Z. Huang, and J. Lin, "Marine environmental monitoring with unmanned vehicle platforms: Present applications and future prospects," *Science of The Total Environment*, vol. 858, p. 159741, 2023.

[27] H. G. Tanner, C. T. Bandara, and M. C. Gyves, "Partial system identification and sensor fusion with the jaiabot micro autonomous underwater vehicle," in *Proceedings of the Mediterranean Conference on Control and Automation*, pp. 167–172, 2024.

[28] C. T. Bandara and H. Tanner, "Marine surface vehicle formations in confined environments," Mar. 2025.

[29] T. I. Fossen, *Handbook of marine craft hydrodynamics and motion control*. John Wiley & Sons, 2011.

[30] D. Pais, P. M. Hogan, T. Schlegel, N. R. Franks, N. E. Leonard, and J. A. R. Marshall, "A mechanism for value-sensitive decision-making," *PloS one*, vol. 8, no. 9, p. e73216, 2013.